Solute transport in nearly saturated porous media under landfill clay liners: A finite deformation approach

H J Zhang[1], D-S Jeng[1,#], D A Barry[2], B R Seymour[3], L Li[4]

[1] *Division of Civil Engineering, University of Dundee, DD1 4HN, UK*
[2] *Laboratoire de technologie écologique, Faculté del'environnement naturel, architectural et construit (ENAC), Station 2, Ecole Polytechnique Fédérale de Lausanne (EPFL), 1015 Lausanne, Switzerland*
[3] *Department of Mathematics, University of British Columbia, Vancouver BC, V6Z 1Z2, Canada*
[4] *National Centre for Groundwater Research and Training, School of Civil Engineering, The University of Queensland, St. Lucia, QLD 4072, Australia*
[#] *Corresponding author, tel: +44(1382) 386141; Fax: +44(1382) 384816; email: d.jeng@dundee.ac.uk*

Abstract

For solute transport in a deformable clay liner, the importance of consolidation in the presence of sorption and consolidation-induced advection are well known. Here a one-dimensional coupled consolidation and solute transport model for a partially saturated porous medium, including the new features of finite strain and geometric and material nonlinearity, is proposed. A new boundary condition at the compacted clay liner (CCL) base is also introduced. A comprehensive comparison demonstrates the significance of finite strain, compressibility of pore water (CPW), longitudinal dispersion (LD) and the degree of saturation on the solute transport in an unsaturated porous medium.

Consolidation in the presence of sorption and consolidation-induced advection both affect solute transport in a deformable clay liner. Here, a one-dimensional coupled consolidation and solute transport model for a nearly saturated porous medium, including finite strain and geometric and material nonlinearity, was proposed. A new boundary condition at the compacted clay liner base was also introduced. The model demonstrates the significance of finite strain, pore water compressibility, dispersion and the degree of saturation on solute transport in an unsaturated, consolidating porous medium.

Keywords: material coordinates; finite deformation; degree of saturation; linear equilibrium sorption; porous flow

---

1. Introduction

Land-based containment facilities are commonly used for the disposal of municipal solid waste and contaminated dredged material (Liu, 2007). In modern landfills, liner systems are designed to isolate the landfill contents from the surrounding environment to protect the groundwater from pollution. For well-constructed composite liners, the geo-membrane typically has few defects, so restricting advection through it (Giroud and Bonaparte, 1989; Foose et al., 2002). However, volatile organic compounds (VOCs) can diffuse through membranes with magnitude four to six orders greater than the possible advection. Therefore, diffusion of VOCs in composite liners is viewed as a critical issue in the design of landfill liners (Foose, 2002).

The VOC transit time was traditionally estimated using the diffusion equation (Rowe and Badv, 1996; Fityus et al., 1999; Foose, 2002). However, several field tests have reported that the transit of VOCs is much earlier than theoretical predictions (Workman, 1993; Othman et al., 1997). Many researchers attribute this to consolidation and associated advective transport. Several theoretical models coupling mechanical consolidation with solute transport were constructed in recent years (Smith, 2000; Fox, 2007; Lewis et al., 2009).

There are opposing opinions regarding the importance of consolidation-induced advection. Based on a model coupling finite deformation consolidation with solute transport, Lewis et al. (2009) claimed that consolidation is essentially complete before the VOC breaks though the clay liner, and its influence is further minimized if sorption occurs. In their illustrative example, with linear sorption at the level of $K_d = 0.001$ l/g, the consolidation made no discernible difference to the concentration at the compacted clay liner (CCL) drainage base. Consequently, they concluded that the advective transport flux has less influence on solute migration than the combination of geometric and void ratio variation. With this assumption, Lewis et al. (2009) proposed several simplified models, such as the *instant deformation-diffusion only* model (calculates the final layer thickness and void ratio before performing a diffusion-only analysis), and the *no advection* model (ignores the advective transport component in the coupled model), to approximate the coupled consolidation and transport model. It is noted that, in their model (Lewis et al., 2009), the boundary condition for the void ratio at the CCL base is constant, which is not consistent with Smith (2000). On the other hand, Fox (2007) presented contrary simulation results and stated that the advective flux caused by consolidation has a lasting effect on transport even after the consolidation has completed, and that its relative importance does not diminish for a VOC sorption level up to 0.001 l/g.

In real environments, the clay barrier below the waste content is not fully saturated (Fityus et al., 1999). Furthermore, when the liner materials are compacted, the required optimal water content will cause the engineered clay to be partially saturated. The optimal water content in compacted clay is close to saturation (Vaughan, 2003). Within a nearly saturated soil, the air phase is not continuous and exists in the form of occluded bubbles (Wang et al., 1997). Soil parameters, such as hydraulic conductivity and effective diffusion, depend on the degree of saturation. Effective diffusion decreases with consolidation. Consequently, the relative importance of the mechanical dispersion component to effective diffusion may reach a level at which it cannot be neglected. Moreover, the compressibility of pore water, which is more pronounced in partially saturated soil (Fredlund and Rahardjo, 1993), has been reported to reduce the rate of porous flows and consolidation (Booker and Carter, 1987; Vaziri and Christian, 1994). Since advective solute transport is induced by pore-water flow, the compressibility of pore water is expected to affect solute migration.

Based on the one-dimensional Biot consolidation theory, Zhang et al. (2012) proposed an advection-diffusion equation that incorporates the degree of saturation, compressibility of the pore fluid (CPW) and dispersivity of the solute transport in a nearly saturated deforming porous medium. Both CPW and dispersivity were found to influence solute migration within the CCL, significantly so in some circumstances. However, Zhang et al. (2012) considered an infinitesimal strain, (i.e., small deformation) model. Additionally, they did not consider the material and geometric nonlinearity, factors that could be important in some circumstances (Lewis et al., 2009). Financial constraints sometimes limit deployment of the relatively costly CCLs. Natural clay deposits (sometimes with relatively high compressibility) are used as substitutes. Since the soft clayey soil generally provides a good contact adhesion with a geomemebrane, high effectiveness is a priori expected. However, the finite deformation caused by the emplacement of waste cannot be neglected.

The objective of this study is to extend the small deformation model for solute transport in a nearly saturated medium (Zhang et al., 2012) to finite deformations. This allows us to clarify the influence of consolidation in the progress of solute transport (using a time-dependent boundary in terms of void ratio at the CCL base). The influence of the degree of saturation on the VOC transit time in clay barriers will also be examined. To account for the geometric nonlinearity, a material coordinate system is used. Both CPW and dispersivity are considered in the new model. Further, our approach incorporates nonlinearity of the constitutive properties related to soil compressibility, the hydraulic conductivity and decreasing effective diffusion coefficient. A parametric study is carried out to examine the influence of several dominant parameters on the process of solute transport in porous medium.

2. Model Formulation

Recently, Lewis et al. (2009) and Peters and Smith (2002) developed a model coupling finite strain consolidation and solute transport in a fully saturated soil. Below, the CPW and dispersion in a nearly saturated soil is included.

2.1. Coordinates systems

A Lagrangian coordinate system (z, t) is employed to derive the flow and transport equations. We define $\xi(z, t)$ as the particle displacement with $\xi(z, 0) = z$. The relationship between Lagrangian and Eulerian (ξ, t) coordinate systems then implies that for any variable $F(z, t) = f(\xi(z, t), t)$:

$$\frac{\partial F}{\partial z} = \frac{\partial f}{\partial \xi}\frac{\partial \xi}{\partial z}, \; \frac{\partial F}{\partial t} = \frac{\partial f}{\partial \xi}\frac{\partial \xi}{\partial t} + \frac{\partial f}{\partial t} = \frac{\partial f}{\partial \xi} v_s + \frac{\partial f}{\partial t}, \tag{1}$$

where $v_s = \partial \xi / \partial t$ is the solid velocity.

2.2. Consolidation equations

The equation describing changes in void ratio, $e(z, t)$, are derived from the continuity equations for the solid and fluid phases together with Darcy's law. The mass balance equation of the solid phase in differential form is::

$$\frac{\partial}{\partial t}\left[\rho_s (1-n) \frac{\partial \xi}{\partial z}\right] = 0, \tag{2}$$

where ρ_s is the soil grain density, $n = e/(1+e)$ is the current porosity, and $n_0 = n(z, 0)$ is the initial porosity. Note that, for constant ρ_s, the Jacobian, M, for the coordinate transformation is:

$$M = \frac{\partial \xi}{\partial z} = \frac{1-n_0}{1-n} = \frac{1+e}{1+e_0}, \tag{3}$$

where e_0 is the initial void ratio.

The continuity equation for the fluid phase (i.e., pore water) is

$$\frac{\partial}{\partial t}\left(nS_r\rho_f \frac{\partial \xi}{\partial z}\right) = -\frac{\partial}{\partial z}(\rho_f q), \tag{4}$$

where ρ_f is the pore fluid density.

According to Darcy's Law, the fluid flux is given by

$$q = -\frac{k_v}{\rho_f g}\frac{\partial p}{\partial \xi}, \tag{5}$$

where k_v is hydraulic conductivity and p is excess pore pressure. If the hydraulic gradient is constant, the Darcy equation in terms of total pressure can be transformed to this form (Peters and Smith, 2002).

Assuming ρ_f varies with pore pressure as $\partial\rho_f/\partial p = \beta\rho_f$ (Barry et al., 2007), substituting Eq. (5) into Eq. (4), then the continuity equation for the fluid phase becomes:

$$nS_r\beta\frac{\partial\xi}{\partial z}\frac{\partial p}{\partial t} + \frac{\partial}{\partial t}\left(S_r\frac{\partial\xi}{\partial z}\right) = \frac{1}{\rho_f g}\frac{\partial}{\partial z}\left(k_v\frac{\partial p}{\partial z}\frac{\partial z}{\partial\xi}\right), \tag{6}$$

where the compressibility of pore fluid (β) can be estimated by (Fredlund and Rahardjo, 1993):

$$\beta = \frac{S_r}{K_{w0}} + \frac{1 - S_r + r_h S_r}{P_a + P_0}, \tag{7}$$

in which K_{w0} is the pore water bulk modulus, r_h denotes volumetric fraction of dissolved air within pore water, P_a denotes gauge air pressure and P_0 represents the atmospheric pressure. In a nearly saturated soil, for example, $r_h = 0.02$, $S_r = 0.8 \sim 1.0, \beta$ falls into the range of $2 \times 10^{-6} \sim 2 \times 10^{-7}$ Pa^{-1}.

Because n and n_0 (implicitly embedded in $\partial\xi/\partial z$) appear simultaneously, and n is unknown, Eq. (6) can not be directly solved in terms of p. In the following derivation, it turns out that once the relationship between the derivative of p (with respect to t and a) and the corresponding derivative of e is known, it is straightforward to convert Eq. (6) to an equation in terms of e.

Assuming self-weight is negligible due to the relatively small thickness of the CCL (Zhang et al., 2012), the vertical force equilibrium is:

$$\frac{\partial\sigma}{\partial z} = 0, \tag{8}$$

where σ (now a function of t only) is the total normal stress of the soil and the z coordinate is vertically upwards. Assuming the compressive normal stress is positive, i.e., $\sigma = \sigma' + p$ (σ' is the effective normal stress), Eq. (8) leads to:

$$\frac{\partial p}{\partial \xi} = \frac{\partial}{\partial z}\left(-\sigma' + \sigma\right)\frac{\partial z}{\partial \xi} = \frac{1+e_0}{1+e}\frac{1}{\alpha_v}\frac{\partial e}{\partial z}, \tag{9}$$

where $\alpha_v = -de/d\sigma'$ is the coefficient of soil compressibility.

In the absence of self-weight, the rate of change of total stress at an arbitrary location equals that of the external top loading,

$$\frac{\partial \sigma}{\partial t} = \frac{\partial Q}{\partial t}, \tag{10}$$

where Q is the external load. The rate of change of the excess pore water pressure in the time domain is:

$$\frac{\partial p}{\partial t} = \frac{\partial}{\partial t}(\sigma - \sigma') = \frac{\partial Q}{\partial t} + \frac{1}{\alpha_v}\frac{\partial e}{\partial t}. \tag{11}$$

Substituting Eq. (3, 9, 11) into Eq. (6) yields:

$$\left(\frac{eS_r\beta}{(1+e_0)\alpha_v} + \frac{S_r}{1+e_0}\right)\frac{\partial e}{\partial t} - \frac{1+e_0}{\rho_f g}\frac{\partial}{\partial z}\left(\frac{k_v}{\alpha_v(1+e)}\frac{\partial e}{\partial z}\right) = -\frac{S_r\beta e}{1+e_0}\frac{\partial Q}{\partial t}. \tag{12}$$

For the fully saturated case and when the CPW is neglected, i.e., $\beta = 0$, Eq. (12) reduces to:

$$\frac{1}{1+e_0}\frac{\partial e}{\partial t} = \frac{1+e_0}{\rho_f g}\frac{\partial}{\partial z}\left(\frac{k_v}{\alpha_v(1+e)}\frac{\partial e}{\partial z}\right), \tag{13}$$

which is identical to Eq. (1) of Lewis et al. (2009).

2.3. Solute transport equations

Solute transport occurs in both solid and fluid phases. Here, for the nearly saturated soil, the mixture of pore water and entrapped air is taken as a homogeneous fluid. Due to the discrete air bubbles, VOC transport by gas diffusion can be neglected in a nearly-saturated soil. Therefore, the mass conservation equation for the solute in the solid phase is:

$$\frac{\partial}{\partial t}\left[(1-n)\rho_s S \frac{\partial \xi}{\partial z}\right] = f'_{a\to s}, \tag{14}$$

where S is the mass of solute sorbed on or within the solid phase per unit mass of the solid phase and $f'_{a\to s}$ denotes rate of solute loss in the water phase by solid phase sorption.

The mass conservation equation for solute in the fluid phase is:

$$\frac{\partial}{\partial t}\left(nS_r c_f \frac{\partial \xi}{\partial z}\right) = -\frac{\partial J_f}{\partial z} - f'_{a\to s}, \tag{15}$$

where c_f is the concentration of the solute in the pore fluid. In Eq. (15), the term $\partial\xi/\partial z$ comes from the volumetric change (Peters and Smith, 2002) and J_f represents solute flux in the fluid phase, which is described by (Peters and Smith, 2002):

$$J_f(z,t) = nS_r(v_f - v_s)c_f - \frac{nS_r D}{M}\frac{\partial c_f}{\partial z}, \tag{16}$$

where D is the hydrodynamic dispersion coefficient. It is given by the sum of the effective diffusion coefficient (D_e) and the coefficient of mechanical dispersion (D_m):

$$D_m = \alpha_L \left(v_f - v_s \right), \tag{17}$$

where α_L is dispersion coefficient, v_f is the pore fluid velocity and $v_f - v_s$ denotes the relative velocity of the pore fluid.

Based on Eq. (14-16), we have:

$$\frac{\partial}{\partial t} \left\{ \left[nS_r c_f + (1-n)\rho_s S \right] \frac{\partial \xi}{\partial z} \right\} = \frac{\partial}{\partial z} \left(\frac{nS_r D}{M} \frac{\partial c_f}{\partial z} \right) - \frac{\partial}{\partial z} \left[nS_r (v_f - v_s) c_f \right]. \tag{18}$$

The above equation can be further simplified with Darcy's Law, Eq. (5), and the mass balance equations for both solid and fluid phases, Eqs. (2) and (4), respectively. Equation (18) can then be expressed as:

$$\begin{aligned} nS_r \frac{\partial \xi}{\partial z} \frac{\partial c_f}{\partial t} + (1-n)\rho_s \frac{\partial \xi}{\partial z} \frac{\partial S}{\partial t} =& \frac{\partial}{\partial z} \left(\frac{nS_r D}{M} \frac{\partial c_f}{\partial z} \right) + \frac{k_v}{\rho_f g} \frac{\partial p}{\partial \xi} \frac{\partial c_f}{\partial z} \\ &+ \left(nS_r \beta \frac{\partial \xi}{\partial z} \frac{\partial p}{\partial t} - \frac{\beta k_v}{\rho_f g} \frac{\partial p}{\partial \xi} \frac{\partial p}{\partial z} \right) c_f. \end{aligned} \tag{19}$$

Substituting Eq. (9) and Eq. (11) into Eq. (19) results in:

$$\begin{aligned} \left(S_r \frac{e}{1+e_0} + \frac{\rho_s K_d}{1+e_0} \right) \frac{\partial c_f}{\partial t} =& S_r \frac{\partial}{\partial z} \left(\frac{e(1+e_0)}{(1+e)^2} D \frac{\partial c_f}{\partial z} \right) + \frac{k_v}{\rho_f g} \frac{1+e_0}{\alpha_v (1+e)} \frac{\partial e}{\partial z} \frac{\partial c_f}{\partial z} \\ &+ \beta \left[S_r \frac{e}{1+e_0} \left(\frac{\partial Q}{\partial t} + \frac{1}{\alpha_v} \frac{\partial e}{\partial t} \right) - \frac{k_v}{\rho_f g \alpha_v^2} \frac{1+e_0}{1+e} \left(\frac{\partial e}{\partial z} \right)^2 \right] c_f, \end{aligned} \tag{20}$$

where K_d describes the partitioning coefficient.

2.4. Special cases

In this section, three special cases of the present model are outlined.

A. Saturated soil with finite deformation

For a saturated soil, where $S_r = 1$, and incompressible pore fluid, i.e., $\beta = 0$, Eq. (20) reduces to:

$$\left(\frac{e}{1+e_0} + \frac{\rho_s K_d}{1+e_0}\right)\frac{\partial c_f}{\partial t} = \frac{\partial}{\partial z}\left(\frac{e(1+e_0)}{(1+e)^2} D \frac{\partial c_f}{\partial z}\right) + \frac{k_v}{\rho_f g}\frac{1+e_0}{\alpha_v(1+e)}\frac{\partial e}{\partial z}\frac{\partial c_f}{\partial z}, \quad (21)$$

which is identical to Eq. (4) of Lewis et al. (2009) and Eq. (44) in Peters and Smith (2002).

B. Small deformation model

Under the assumptions of negligible self-weight and small deformation (constant porosity, i.e., $n = n_0$), the coupled small deformation model is (Zhang et al., 2012):

$$S_r n_0 \beta \frac{\partial p}{\partial t} + S_r \frac{\partial^2 u}{\partial t \partial \xi} = \frac{1}{\rho_w g}\frac{\partial}{\partial \xi}\left(k_v \frac{\partial p}{\partial \xi}\right), \quad (22)$$

$$G\frac{2(1-\nu)}{(1-2\nu)}\frac{\partial^2 u}{\partial \xi^2} = \frac{\partial p}{\partial \xi} \quad (23)$$

and:

$$\begin{aligned}
\left[S_r n_0 + (1-n_0)\rho_s K_d\right]\frac{\partial c_f}{\partial t} = {} & S_r n_0 D_e \frac{\partial^2 c_f}{\partial \xi^2} - \alpha_L \frac{k_v}{\rho_w g}\frac{\partial p}{\partial \xi}\frac{\partial^2 c_f}{\partial \xi^2} \\
& + \frac{\partial c_f}{\partial \xi}\left\{-\alpha_L S_r n_0 \beta \frac{\partial p}{\partial t} - \alpha_L S_r \frac{\partial^2 u}{\partial \xi \partial t}\right. \\
& + \frac{\alpha_L \beta k_v}{\rho_w g}\left(\frac{\partial p}{\partial \xi}\right)^2 + S_r D_e (1-n_0)\frac{\partial^2 u}{\partial \xi^2} \\
& \left. + \frac{k_v}{\rho_w g}\frac{\partial p}{\partial \xi} - \left[S_r n_0 + (1-n_0)\rho_s K_d\right]\frac{\partial u}{\partial t}\right\} \\
& + S_r n_0 \beta \frac{\partial p}{\partial t} c_f - \beta \frac{k_v}{\rho_w g}\left(\frac{\partial p}{\partial \xi}\right)^2 c_f + S_r n_0 \beta \frac{\partial u}{\partial t}\frac{\partial p}{\partial \xi} c_f,
\end{aligned} \quad (24)$$

where u is the soil displacement, G the shear modulus and ν Poisson's ratio. The constant material coefficients can be described as:

$$G = \frac{c_v \rho_f g(1-2\nu)}{2k_v(1-\nu)} = \frac{(1+e_p)(1-2\nu)}{2(1-\nu)\alpha_{vp}}, \\ k_v = k_p, \quad D_e = D_{e0}, \tag{25}$$

where c_v is the consolidation coefficient; k_s and k_p the saturated hydraulic conductivity and hydraulic conductivity of the soil corresponding to e_p (the void ratio corresponding to pre-consolidation stress), respectively.

C. Nearly saturated soil with no deformation

For the partially saturated no deformation model, i.e., $e = e_0$, $\xi = z$, the overloading, Q, does not affect solute transport. In the spatial coordinate system (ξ, t), Eq. (20) reduces to the linear diffusion equation:

$$\frac{\partial c_f}{\partial t} = D\left(1 + \frac{\rho_s K_d}{S_r e_0}\right)^{-1} \frac{\partial^2 c_f}{\partial \xi^2}. \tag{26}$$

3. Variations of parameters in consolidation and solute transport processes

The finite deformation model allows consideration of the effects of variations in the coefficients of consolidation and transport (such as the coefficient of compressibility, α_v, hydraulic conductivity, k_v and hydrodynamic dispersion, D) on solute transport process. Lewis et al. (2009) utilized void ratio-dependent functions for the related coefficients while Li and Liu (2006) used a fractal pore-space theory to develop fractal models of water flow and solute diffusion in rigid unsaturated soils. Their approach allowed comparison of these coefficients between the fully saturated and unsaturated cases. Here, a combination of both models is employed so that the hydraulic conductivity and the effective diffusion depend on both the void ratio and the degree of saturation. Linear, reversible solute sorption is assumed in this study; however, the approach can be adapted for other sorption models.

3.1. Soil compressibility

The soil layer is assumed to be over-consolidated, and compression of the soil layer commences when the applied stress exceeds the pre-consolidation stress, i.e., deformation due to re-compression is neglected. In this case, the void ratio is idealized as a linear function of the logarithm of the effective stress (Means and Parcher, 1964):

$$e = e_p - C_c \log\left(\frac{\sigma'}{\sigma'_p}\right), \tag{27}$$

where σ' is effective stress, σ'_p denotes the pre-consolidation stress and C_c is the compression index of the soil (defined by the absolute value of the slope of the idealized virgin compression line). For a nearly saturated soil, the degree of saturation is sufficiently high so that the air phase exists in the form of occluded bubbles. Vaughan (2003) claimed that the presence of occluded air bubbles is unlikely to affect soil effective stresses. Therefore, Eq. (27) is employed to describe the volumetric change of a nearly saturated soil.

The coefficient of compressibility in terms of void ratio can be obtained by differentiation of Eq. (27) with respect to effective normal stress (Lewis et al., 2009):

$$\alpha_v = \alpha_{vp}\exp\left[\ln 10\left(\frac{e-e_p}{C_c}\right)\right], \tag{28}$$

where α_{vp} is the coefficient of compressibility corresponding to σ'_p, i.e.,

$$\alpha_{vp} = \frac{C_c}{\sigma'_p \ln 10}. \tag{29}$$

3.2. Hydraulic characteristic

For hydraulic conductivity, an empirical relationship describing its variation with void ratio in saturated clay soils is given as (Mitchelll, 1993)::

$$k_s = k_p\exp\left[\ln(10)\left(\frac{e-e_p}{C_k}\right)\right], \tag{30}$$

where C_k is the hydraulic conductivity index.

The power law relationship equation for hydraulic conductivity versus water content θ (= $S_r n$) is (Li and Liu, 2006):

$$k_v = k_s\left(\frac{\theta}{\theta_s}\right)^{\alpha}, \tag{31}$$

where θ_s is saturated water content, and α falls in the range of 2.68 to 2.78 for clay loam.

3.3. Dispersion coefficient

In a saturated soil, the effective solute diffusion coefficient is defined as the product of the free diffusion coefficient of the solute in the pore fluid (D_f) and the tortuosity factor (t_f), which accounts for the irregular path that diffusing molecules must take through the pore space (Acar and Haider, 1990). Lewis et al. (2009) claimed that it is rational to take D_e as constant, because uncertainty of the range of τ_f can be the same order of consolidation-induced change of D_e. Alternatively, the reduction of D_e can be expressed with a hypothetical relationship associated with the overall void ratio change as (Lewis et al., 2009; Morel-Seytour et al. , 1996):

$$D_e = \left(\frac{e_0 - e}{3(e_0 - e_f)} + \frac{e - e_f}{e_0 - e_f} \right) D_{e_0}, \tag{32}$$

where e_f denotes the final void ratio, and D_{e0} is the initial effective dispersion coefficient.

In variably saturated soils, the effective diffusion coefficient, D_e, depends on soil water content, bulk density, and soil type for soils with different textures. Regarding the water content, there is a threshold value under which solute diffusivity vanishes (Hunt and Ewing, 2003; Hamamoto et al., 2009). The impedance factor (Porter et al., 1960) (i.e., the ratio of solute diffusion coefficient in soil to product of solute diffusion coefficient in free water and volumetric soil water content), decreased with increasing bulk density for each soil type, but the effect of the overall bulk density on the impedance factor is minor compared with the effect of soil water content and soil type (Hamamoto et al., 2009). The effective diffusion coefficient was found to decrease with decreasing saturation in laboratory experiments (Barbour et al., 1996). The decrease was found to be quite rapid initially, followed by a near-linear decline for degree of saturation below 60%. Here, the soil diffusion coefficient is expressed as (Li and Liu, 2006)::

$$D_e = 1.1 D_f \theta(\theta - \theta_t), \tag{33}$$

where θ_t denotes threshold water content, which was observed to become higher with increasing clay content and varies between 3% and 20% for clay soil.

3.4. Sorption

It has been reported that the effect of the degree of saturation on the adsorption coefficient is insignificant from full saturation to a degree of saturation of 10% (Barbour et al., 1996). A significant decrease in the adsorption coefficient only occurs in cases with a low degree of saturation. In this study the degree of saturation varies from 1 to 0.8, i.e., the effect on sorption can be neglected. Therefore, the concentration of solute in the solid phase, S, is expressed as:

$$S = K_d c_f. \tag{34}$$

This assumption of a linear sorption is valid at the relatively low concentrations that are usually found in the municipal waste disposal sites (Mathur and Jayawardena, 2008).

4. Application to a landfill liner

4.1. Problem description

As the schematic in Fig. 1 shows, the composite landfill liner beneath a primary leachate collect system (PLCS) consists of an impermeable (to diffusion of inorganic solute) geomembrane, an underlying engineered compacted clay layer (CCL), and a second leachate collecting system (SLCS).

The model parameters employed in the following analyses are based on those used in recent studies of solute transport in composite liners (Foose, 2002; Lewis et al., 2009). Because of the unavailability of consolidation data in the literature, hypothetical values of the applied stress, pre-consolidation stress, compression index, hydraulic conductivity index, threshold moisture content and other parameters in calculating the D_e and k_v are used. As a primary parameter, the compression index covers a large range to account for the high-compressibility soil considered (Lewis et al., 2009). However, the related applied stress was selected to avoid negative and unrealistically low void ratios. The parameters used are given in Table 1.

4.2. Boundary conditions for consolidation

The following boundary conditions are introduced. Assuming there are no defects in the geomembrane, the top boundary ($z = 0$) is assumed to be impermeable, i.e., $q = 0$. Therefore, from Eq. (5) and Eq. (9),

$$\frac{\partial e}{\partial z} = 0 \text{ at } z = 0. \tag{35}$$

At the bottom drainage boundary ($z = L$), the excess pore pressure is zero and a Dirichlet-type boundary condition for void ratio (e) can be derived from the effective stress–void ratio equilibrium relationship, Eq. (27):

$$e = e_p - C_c \log\left(\frac{\sigma'_L}{\sigma'_p}\right), \tag{36}$$

where σ'_L denotes the effective stress at bottom.

The excess pore pressure vanishes at the bottom boundary, so $\sigma'_L = \sigma_a$, where σ_a is a time-varying stress due to the external overburden. Note that σ_a is the maximum loading in the model of Lewis et al. (2009). The void ratio rapidly approaches a steady value, which consequently leads to a spurious higher fluid velocity and faster solute transportation. To distinguish the cases, we label the present boundary condition at the CCL bottom as 'BCC' and 'BCL', i.e., the boundary conditions used by Lewis et al. (2009).

4.3. Boundary conditions for solute transport

At the top of the CCL, VOC diffusion through the geo-membrane is described by Fick's law (Booker et al., 1997), so the concentration gradient is proportional to the difference in concentrations on each side of the (sufficiently thin) geomembrane. In the material coordinate system, the boundary condition is (Lewis et al., 2009):

$$\frac{\partial c_f}{\partial z}(0,t) = \frac{(1+e(0,t))^2}{e_0(1+e_0)}\frac{P_G}{hD_e}\left(c_f(0,t) - C_{f0}\right), \tag{37}$$

where C_{f0} is the (constant) solute concentration at the top surface of the geo-membrane with the assumption that the landfill waste volume is large (Peters and Smith, 2002); h and P_G are, respectively, the thickness and the permeation coefficient for the solute in the geo-membrane.

The lower boundary condition for the solute concentration (c_f) is (Peters and Smith, 2001):

$$\frac{\partial c_f}{\partial z} = 0, \text{ at } z = L, \tag{38}$$

which assumes negligible diffusion below the CCL base (Barry and Sposito, 1988).

5. Numerical results and discussion

A numerical solution was constructed using COMSOL 3.5a (Comsol, 2010). It discretized the domain into unstructured Lagrange-linear elements with a maximum global element size of 10^{-2} m, and maximum local element size at the end boundaries (where the most rapid changes occur) of 10^{-4} m. Temporally, the subtime step was 10^{-2} y. To be easily interpreted, solution curves were plotted in the spatial coordinate x:

$$x = z + \int_{z}^{L} \frac{e_0 - e(\zeta)}{1 + e_0} d\zeta. \tag{39}$$

Thus, the first-order PDE,

$$\frac{\partial x}{\partial z} = 1 - \frac{e_0 - e(z)}{1 + e_0}, \tag{40}$$

with boundary conditions $x(0,t) = S_{mt}$ and $x(L,t) = L$ was constructed to find x, where the settlement S_{mt} is given by:

$$S_{mt} = \int_{0}^{L} \frac{e_0 - e(\zeta)}{1 + e_0} d\zeta. \tag{41}$$

5.1. Model verification

Since there are no experimental data available in the literature, the present model was reduced to the full-saturation case using the same boundary condition at the CCL bottom for e as used by Lewis et al. (2009), i.e., σ_a is taken as the maximum loading; and $K_d = 0$, $\alpha_L = 0$, $C_c = 0.8$, $k_p = 10^{-9}$ m/s. A comparison between the present and previous models is illustrated in Fig. 2. In the figure, the results of the finite deformation with constant and decreasing hydrodynamic dispersion, Eq. (32), small deformation model (Zhang et al., 2012) and the pure diffusion model (i.e., no deformation model) are included. Both consolidation (i.e., void ratio, e, distribution) and relative concentration obtained from the present model are in excellent agreement with results of Lewis et al. (2009). As shown in Fig. 2, with the constant effective diffusion coefficient, the small deformation model (Zhang et al., 2012) predicts a slower solute migration than the corresponding finite deformation model.

5.2. Correctness of the boundary condition at CCL base

The differences due to the different boundary conditions, 'BCL' (used by Lewis et al. (2009)) and 'BCC' (used in the present model), are presented in Fig. 3, where $C_c = 0.8$ and $k_p = 10^{-9}$ m/s. A comparison of Fig. 3(a) (BCC) and 2(a) (BCL) shows that taking σ_a as the maximum loading leads to a greater void ratio gradient and a faster consolidation process, although the final value of e is very close. This initially speeds up the solute transit slightly, and then slows it down in the long-term (Fig. 3(b)). The reason the trend reverses after the consolidation completes for the 'BCL' case is that the higher solute concentration level during the consolidation phase of 'BCC' occurs later resulting in an increased advective flux. The separation is more obvious for the relatively soft and higher permeablility cases. In the following sections all numerical results are based on the boundary condition 'BCC'.

5.3. Effect of consolidation

On basis of the 'BCL' boundary condition, Lewis et al. (2009) observed that there is no noticeable solute concentration at the CCL base when consolidation of the liner is completed even for the case of very high compressibility ($C_c = 0.8$). They thus concluded that transport can be simulated using the pure diffusion model with the final void ratio value. However, during consolidation the distribution of solute concentration changes, which is the initial condition of what follows. Thus, advective transport due to consolidation may not be negligible.

Figures 4 and 5 illustrate the consolidation processes and solute transport in a saturated soil for two cases with different compression indices (C_c) and hydraulic conductivities (k_v). Consolidation lasts 2.2 and 34.5 y for $C_c = 0.2$ and $C_c = 0.8$, respectively. For the 'soft' case, a noticeable concentration difference from the no deformation model appears at the CCL base during consolidation, as shown in Fig. 5. The difference decreases with higher levels of sorption (Fig. 5(b)). The effect of consolidation on transport exists during both the consolidation and post-consolidation stages, which is consistent with Fox (2007). Since the advection results in a notable concentration level at the CCL base, simplifying assumptions such as instant deformation, pure diffusion and finite deformation without advection modelling are not appropriate. The magnitude of solute concentration C_f in Fig. 5(a) is an order greater than that in Fig. 5(b). Here, the influence of sorption is noticeable as it drastically retards the solute transport.

Figures 6 and 7 present the results for a nearly saturated soil. We see again that soft clay consolidation has a noticeable effect on solute transport (Fig. 6). However, since the effective diffusion (D_e) reduces with deformation, concentrations for the pure diffusion model surpass those of coupled models, as is obvious for the case of $K_d = 1$ ml/g.

Consolidation effects are composed of the variation of void ratio and the occurrence of pore water flow, which in turn causes the advective transport flux. As mentioned previously, Lewis et al. (2009) claimed the advection component can be ignored as long as the variation of void ratio is considered. Here, we included in Fig. 8 the case of finite deformation without advection, i.e., advection is removed from Eq. (20). Exclusion of advection underestimates the concentration level and consequently leads to a longer transit time. In the absence of sorption, at the nominal 10% breakthrough, a nearly twofold change occurs in the transit time; this change increases when sorption is included.

5.4. *Effect of degree of saturation*

Fig. 9 demonstrates that the higher saturation of the no-deformation (ND) model results in faster solute transport due to the saturation (S_r)-dependent effective diffusion; the gap is larger in the presence of sorption. Concentrations predicted by the coupled finite deformation and solute transport model are shown in Figures 10 and 11. For cases with parameters $C_c = 0.8$ and $k_p = 10^{-9}$ m/s, consolidation lasts for approximately 12.8 y. Higher saturation results in faster solute transport because of greater effective diffusion, regardless of the sorption. For decreasing D_e, the transit time increases. With sorption, finite deformation with $S_r = 0.8$ and constant D_e leads to almost the same concentration as for the ND model (Fig. 11(b)). Again, this demonstrates that the effect of unsaturation is more apparent in the presence of sorption. Interestingly, with both sorption and decreasing D_e taken into account, finite deformation (FD) models will not always produce faster solute transport (Fig. 10(b)). During consolidation and in the early post-consolidation stage, the FD models have a faster transit, but then are surpassed by the ND model because the effective diffusion is reduced due to compaction. However, the decreasing D_e with compaction is inevitable. In the field, VOC has been shown to appear earlier than predicted by the pure diffusion model has been observed (Peters and Smith, 2002). Possible explanations are: (1) the constitutive relationships for soil parameters are not accurate enough; or (2) other factors, such as heat transfer, should be also included in the model.

5.5. Effects of compressibility of pore water (CPW)

As shown in Fig. 12, the effect of compressibility of pore water (CPW) is related to the soil consolidation coefficient. The influence of CPW on the relative concentration at the CCL becomes more significant for the cases with smaller consolidation coefficients. When the soil is relatively soft ($C_c = 0.8$ and $k_p = 2\times10^{-10}$ m/s), CPW causes twofold longer transit times for the nominal 10% breakthrough. However, at the early consolidation stage, the retarding effect of CPW is more pronounced for 'stiffer' soils and then the trend reverses (Fig. 12) after consolidation completes. These graphs are not shown as the numerical values are too small to present in the same figure. This can be explained by the slowing fluid flow and longer consolidation time due to CPW. Since the separation of curves at a relatively higher concentration level, i.e., absolute concentration difference, is of interest, it follows that the influence of CPW is more significant in softer soil.

To investigate further the influence of CPW, three models examining the three terms containing β are considered here.

- Model A: eliminate $\frac{eS_r\beta}{(1+e_0)\alpha_v}\frac{\partial e}{\partial t}$ from Eq. (12);
- Model B: eliminate $-\frac{S_r\beta e}{1+e_0}\frac{\partial Q}{\partial t}$ from Eq. (12);
- Model C: eliminate the term involving β from Eq. (20).

As shown in Fig. 13, each of the missing terms leads to a large deviation from the full model, so all terms involving β should be retained for the cases considered.

5.6. *Effect of dispersion*

Lewis et al. (2009) neglected mechanical dispersion on the assumption that the pore fluid velocity in fine-grain soil is less than 10^{-6} m^2/s. However, as shown in Fig. 14, its influence cannot be neglected when the clay is relatively soft, even when the maximum fluid average linear velocity is approximately 4.5×10^{-9} m/s for the case $C_c = 0.8$ and $k_p = 2 \times 10^{-10}$ m/s. Its influence becomes more significant as the hydraulic conductivity increases with the same soil compressibility, C_c. This is because decreasing D_e increases the Péclet number (ratio of the rate of advection to the rate of diffusion). Therefore, a rough estimate using pore fluid velocity alone as proposed by Lewis et al. (2009) is not always definitive.

Figure 15 illustrates the individual influence of decreasing D_e, dispersion and CPW. The effect of reducing D_e causes slower transport, while dispersion a faster transit. Although the influence of CPW is not as significant as decreasing D_e and dispersion, it is not negligible, as shown in Fig. 15.

5.7. *Effect of finite deformation*

For the soil without sorption (see Fig. 2b, 10a, 11a, 15a), the ND model always leads to a longer transit time than the finite deformation model. In the presence of sorption (as shown in Fig. 11b), the difference between the ND model and the finite deformation model is negligibly small. However, when the decrease of the effective diffusion coefficient due to deformation is also considered (Fig. 10b and 15b), the results of the two models differ.

Compared with the finite deformation model, the small deformation model can overestimate the contaminant transit time in a liner undergoing large consolidation (Fig. 2b). This demonstrates that the significance of geometric nonlinearity is noticeable for relatively soft soil. This finding is consistent with that of Peters and Smith (2002) and Lewis et al. (2009). Regarding the consolidation, the small deformation model can predict settlement that is non-physical for soft soil (i.e., larger than the total soil thickness). Therefore, for a relatively compressible soil, where the consolidation effect is more significant, a finite deformation consolidation is necessary when being coupled with the solute transport.

6. Conclusion

In this paper, a finite deformation model for coupling consolidation and solute transport processes in partially saturated soil has been presented. It was applied to predict the VOC breakthrough in a landfill clay liner. CPW, dispersion, the non-linear variation of soil compaction, hydraulic conductivity and effective diffusion are included in the model. Based on the numerical simulation results, we conclude that:

1. Consolidation-induced advection has a lasting effect on solute transport during and after the deformation for relatively compressible soil regardless of the sorption level, though the sorption can dramatically slow the solute transport process rate.

2. After an initial acceleration effect on transport, the finite-deformation coupled model with decreasing effective diffusion and sorption produces a lower concentration at the CCL base than the pure diffusion model.

3. A lower degree of saturation leads to a slower pore fluid flow and solute transport(since larger pores drain preferentially with decreasing saturation). The CPW associated with unsaturated conditions cannot be ignored when the consolidation is required to be coupled with solute transport. In the

model, CPW terms exist in both the consolidation and transport equations, none of which can be neglected for simplification. Effective diffusion decreases during consolidation and consequently the relative importance of mechanical dispersion becomes profound. For a long-term prediction, mechanical dispersion could cause significant solute transport. Therefore, it should be included in modelling efforts.

4. Generally speaking, reducing soil compressibility and improving sorption levels of clay are the most effective ways to retard contaminant migration. At the same level of stiffness and sorption, the lower hydraulic conductivity and lower degree of saturation can lengthen the time for contaminants to break through the protective liner.

References

Acar, Y. B., Haider, L., 1990. Transport of low-concentration contaminants in saturated earthen barriers. Journal of Geotechnical Engineering, ASCE 116 (7), 1031–1052.

Barbour, S. L., Lim, P. C., Fredlund, D. G., 1996. A new technique for diffusion testing of unsaturated soil. American Society for Testing and Materials 19 (3), 247–258.

Barry, D. A., Sposito, G., 1988. Application of the convection-dispersion model to solute transport in finite soil columns. Soil Science Society of America Journal 52 (1), 3–9.

Barry, D. A., Lockington, D. A., Jeng, D.-S. , Parlange, J.-Y., Li, L., and Stagnitti, F., 2007. Analytical approximations for flow in compressible, saturated, one-dimensional porous media. Advances in Water Resources. 30 (4), 927–936.

Booker, J. R., Carter, J. P., 1987. Withdrawal of a compressible pore fluid from a point sink in an isotropic elastic half space with anisotropic permeability. International Journal of Solids and Structures 23 (3), 369–385.

Booker, J. R., Quigley, R. M., Rowe, R. K., 1997. Clayey Barrier Systems for Waste Disposal Facilities. Spon Press, London.

Comsol, 2010. COMSOL Multiphysics. 3rd Edition.

Fityus, S. G., Smith, D. W., Booker, J. R., 1999. Contaminant transport through an unsaturated soil liner beneath a landfill. Canadian Geotechnical Journal 36 (2), 330–354.

Foose, G. J., 2002. Transit-time design for diffusion through composite liners. Journal of Geotechnical and Geoenviromental Engineering, ASCE 128 (1), 590–601.

Foose, G. J., Benson, C. H., Edil, T. B., 2002. Comparison of solute transport in three composite liners. Journal of Geotechnical and Geoenviromental Engineering, ASCE 128 (5), 391–403.

Fox, P., 2007. Coupled large strain consolidation and solute transport.ii: Model verification and simulation results. Journal of Geotechnical and Geoenvironmental Engineering, ASCE 133 (1), 16–29.

Fredlund, D., Rahardjo, H., 1993. Soil mechanics for unsaturated soils. John Wiley and Sons, New York.

Giroud, J., Bonaparte, R., 1989. Leakage through liners constructed with geomembranes–Part I. Geomembrane liners. Geotextiles and Geomembranes 8 (1), 27 – 67.

Hamamoto, S., Perera, M. S. A., Resurreccion, A., Kawamoto, K., Hasegawa, S., Komatsu, T., Mldrup, P., 2009. The solute diffusion coefficient in variably compacted, unsaturated volcanic ash soils. Vadsoe Zone Journal, Soil Science Society of America 8 (4), 942–952.

Hunt, A. G., Ewing, R. P., 2003. On the vanishing of solute diffusion in porous media at a threshold moisture content. Soil Science Society of America Journal 67, 1701–1702.

Lewis, T. W., Pivonka, P., Smith, D. W., 2009. Theoretical investigation of the effects of consolidation on contaminant transport through clay barriers. International Journal for Numerical and Analytical Methods In Geomechanics 33, 95–116.

Li, S., Liu, Y., 2006. Application of fractal models to water and solute transport in unsaturated soils. In: Advances in Unsaturated Soil, Seepage, and Environmental Geotechnics (GSP 148), Proceedings of Sessions of GeoShanghai, Shanghai, China, 195-202..

Liu, W.-L., 2007. Thermal analysis of landfills. Ph.D. Thesis, Wayne State University, Detroit, USA

Mathur, S., Jayawardena, L. P., 2008. Thickness of compacted natural clay barriers in msw landfills. Practice Periodical of Hazardous, Toxic, and Radioactive Waste Management, ASCE 12 (1), 53–57.

Means, R. E., Parcher, J. V., 1964. Physical Properties of Soils. Constable and Company Ltd., London.

Mitchelll, J. K., 1993. Fundamentals of Soil Behaviour. Wiley, New York.

Morel-Seytour, H. J., Meyer, P. D., Touma, J., van Genuchten, M. T., and Lenhard, R. J., 1996. Parameter equivalence for the Brooks-Corey and van Genuchten soil characteristics: Preserving the effective capillary drive. Water Resources Research 32 (5), 1251–1258.

Othman, M. A., Bonaparte, R., Gross, B. A., 1997. Preliminary results of composite liner field performance study. Geotextiles and Geomembranes 15 (4-6), 289–312.

Peters, G. P., Smith, D. W., 2001. Numerical study of boundary conditions for solute transport through aporous medium. International Journal for Numerical and Analytical Methods in Geomechanics 25 (7), 629–650.

Peters, G. P., Smith, D. W., 2002. Solute transport through a deforming porous medium. International Journal for Numerical and Analytical Methods in Geomechanics 26 (7), 683–717.

Porter, L., Kemper, W., Jackson, R., and Stewart, B. A., 1960. Chloride diffusion in soils as influenced by moisture content. Soil Science Society of America. Proceedings 24, 460–463.

Rowe, R., Badv, K. ., 1996. Advective-diffusive contaminant migration in unsaturated sand and gravel. Journal of Geotechnical Engineering, ASCE 122, 965–975.

Smith, D. W., 2000. One-dimensional contaminant transport through a deforming porous medium: Theory and a solution for a quasi-steady-state problem. International Journal for Numerical and Analytical Methods in Geomechanics 24 (8), 693–722.

Vaughan, P. R., 2003. Observations on the behaviour of clay fill containing occluded air bubbles. Géotechnique 53 (2), 265–272.

Vaziri, H. H., Christian, H. A., 1994. Application of terzaghi's consolidation theory to nearly saturated soils. Canadian Geotechnical Journal 31 (2), 311–317.

Wang, Z., Feyen, J., Nielsen, D. R., van Genuchten, M. T., 1997. Two-phase flow infiltration equations accounting for air entrapment effects. Water Resources Research 33 (12), 2759–2767.

Workman, J. P., 1993. Interpretation of leakage rates in double-liner systems. In: Koerner, R. M., R F Wilson-Fahmy, R. F. (Eds.), Geosynthetic liner systems: Innovations, concerns, and designs. Industrial Fabrics Association International, pp. 95–112.

Zhang, H. J., Jeng, D.-S., Seymour, B. R., Barry, D. A., Li, L., 2012. Solute transport in partially-saturated deformable porous media: Application to a landfill clay liner. Advances in Water Resources 40, 1–10.

List of symbols

z, material coordinate, L

C_c, compression index of the soil

C_k, hydraulic conductivity index

c_{f0}, solute mass concentration at top of geo-membrane, $\mathrm{ML^{-3}}$

c_f, concentration of the solute in the fluid phase, $\mathrm{ML^{-3}}$

c_s, concentration of the solute in the solid phase, $\mathrm{ML^{-3}}$

D, hydrodynamic dispersion coefficient, $\mathrm{L^2T^{-1}}$

e, void ratio

e_0, initial void ratio

e_p, void ratio corresponding to the pre-consolidation stress

P_G, mass transfer coefficient of geomembrane, $\mathrm{L^2T^{-1}}$

D_e, effective diffusion coefficient, $\mathrm{L^2T^{-1}}$

D_{e0}, initial effective dispersion coefficient, $\mathrm{L^2T^{-1}}$

D_f, free diffusion coefficient of the solute in the pore fluid, $\mathrm{L^2T^{-1}}$

D_m, coefficient of mechanical dispersion, $\mathrm{L^2T^{-1}}$

$f_{a\to s}$, rate of solute loss in aquatic phase by sorption onto solid phase, $\mathrm{ML^{-3}T^{-1}}$

G, shear modulus of soil, $\mathrm{ML^{-1}T^{-2}}$

g, gravity acceleration, $\mathrm{LT^{-2}}$

h, thickness of geomembrane, L

J_f, solute flux in fluid phase, $\mathrm{M^2L^{-3}T^{-1}}$

k_p, hydraulic conductivity corresponding to e_p, $\mathrm{LT^{-1}}$

k_s, saturated hydraulic conductivity, $\mathrm{LT^{-1}}$

k_v, hydraulic conductivity, $\mathrm{LT^{-1}}$

K_d, contaminant partitioning coefficient, $\mathrm{L^3M^{-1}}$

K_{w0}, pore water bulk modulus, $\mathrm{ML^{-1}T^{-2}}$

L, thickness of CCL, L

M, Jacobian of coordinate transformation

n, current soil porosity

n_0, initial soil porosity

P_a, atmospheric pressure, $ML^{-1}T^{-2}$

P_0, atmosphere air pressure, $ML^{-1}T^{-2}$

p, excess pore pressure, $ML^{-1}T^{-2}$

r_h, volumetric fraction of dissolved air

q, Darcy flow velocity, LT^{-1}

Q, external load, $ML^{-1}T^{-2}$

S, mass of contaminant sorbed onto the solid phase per unit mass of solid phase

S_r, degree of saturation

t, time, T

u, soil displacement, L

u', arbitrary variable

U, arbitrary variable

v_f, average fluid velocity, LT^{-1}

v_s, solid velocity, LT^{-1}

x, spatial coordinate, L

598 **Greek symbols**

ξ, spatial coordinate, L

τ_f, the tortuosity factor

σ, total soil stress, $ML^{-1}T^{-2}$

$\sigma^{'}$, effective soil stress, $ML^{-1}T^{-2}$

σ_a, the time varying stress due to external overburden, $ML^{-1}T^{-2}$

σ'_L, the effective stress at bottom, $ML^{-1}T^{-2}$

σ'_p, effective soil stress corresponding to the pre-consolidation stress

ρ_f, density of pore water, ML^{-3}

ρ_s, density of soil gain, ML^{-3}

β, compressibility of pore water, LT^2M^{-1}

ν, Poisson's ratio

α, coefficient in calculating k_v

α_L, longitudinal dispersion, L

α_v, coefficient of compressibility, LT^2M^{-1}

α_{vp}, coefficient of compressibility corresponding to σ'_p, LT^2M^{-1}

θ, water content

θ_s, saturated water content

θ_t, threshold water content

List of Tables

Table 1: Values of input parameters

Parameter	Value
Maximum applied stress (ramp loading for 2 years), σ_a	450 kPa
Preconsolidation stress, σ'_p	50 kPa
Compression index, C_c	0.2, 0.8
Preconsolidation hydraulic conductivity, k_p	10^{-9}, 2×10^{-10} m/s
Constant, α	2.7
Hydraulic conductivity index, C_k	0.585
Thickness of geomembrane, h	0.0015 m
Thickness of CCL, L	1.22 m
Mass transfer coefficient of geomembrane, P_G	4×10^{-11}m^2/s
Initial effective diffusion coefficient, D_{e0}	2×10^{-10} m^2/s
Free diffusion coefficient in the pore fluid, D_f	10^{-9} m^2/s
Threshold moisture content, θ_t	0.05
Partitioning coefficient, K_d	0, 0.2, 1 ml/g
Dispersion, α_L	0, 0.1 m
Initial void ratio, e_0 ($= e_p$)	1.17
Acceleration due to gravity, g	9.81 m/s^2
Initial density of pore water, ρ_f	10^3 kg/m^3
Density of the solid phase, ρ_s	2.7×10^3 kg/m^3
Degree of saturation of clay, S_r	1, 0.9, 0.8

List of Figures

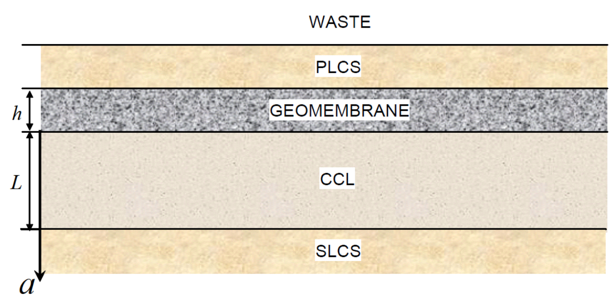

Figure 1: A Schematic of a composite landfill liner

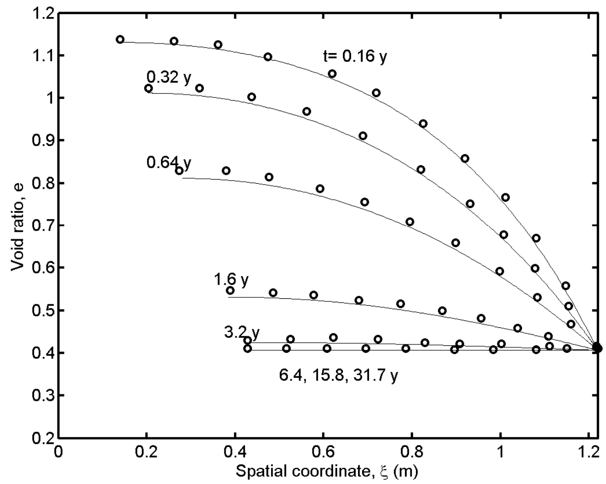

(a) Void ratio evolution

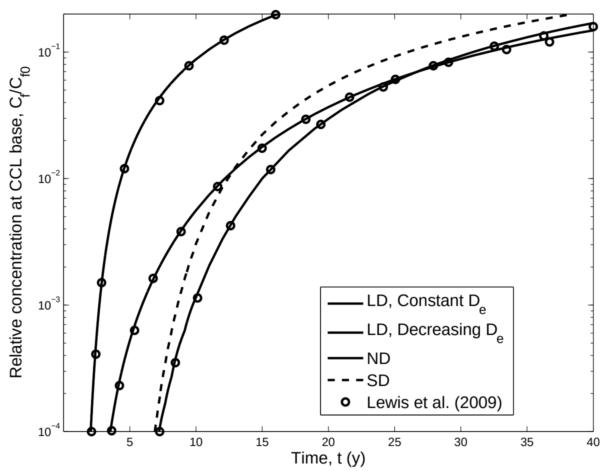

(b) Breakthrough curves

Figure 2: Comparison of (a) void ratio evolution and (b) breakthrough curves between the present model (solid line) and Lewis et al. (2009) (circle). Notations: FD: finite deformation model, SD: small deformation model, ND: no deformation model.

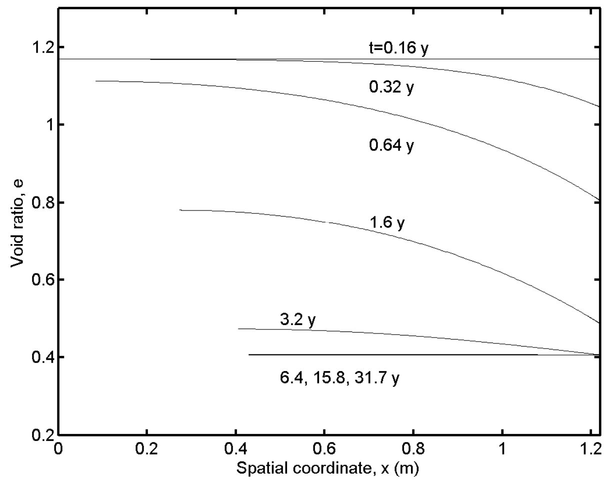

(a) Void ratio evolution (BCC only)

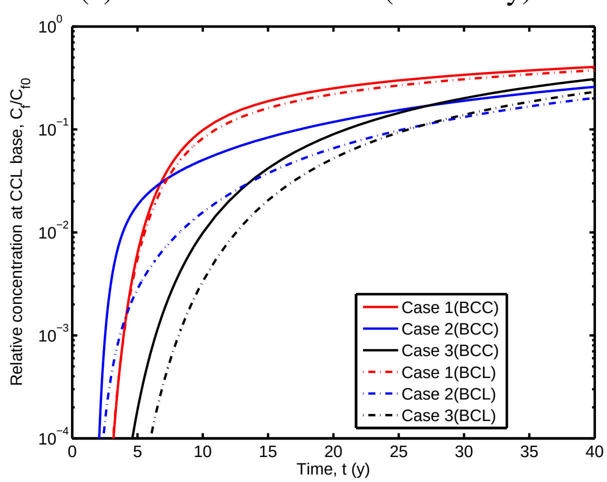

(b) Breakthrough curves (BCC and BCL)

Figure 3: Influence of Boundary condition of void ratio (e) at CCL base (a) void ratio evolution (BCC only) and (b) breakthrough curves ($S_r = 1$, $\beta = 0$, $\alpha_L = 0$, constant D_e). In (b), solid line for 'BCC', and dash-dot line for 'BCL'. Case 1: $k_p = 2 \times 10^{-10}$ m/s, C_c =0.8; Case 2: $k_p = 10^{-9}$ m/s, C_c =0.8; and Case 3: $k_p = 10^{-9}$ m/s, C_c =0.2.

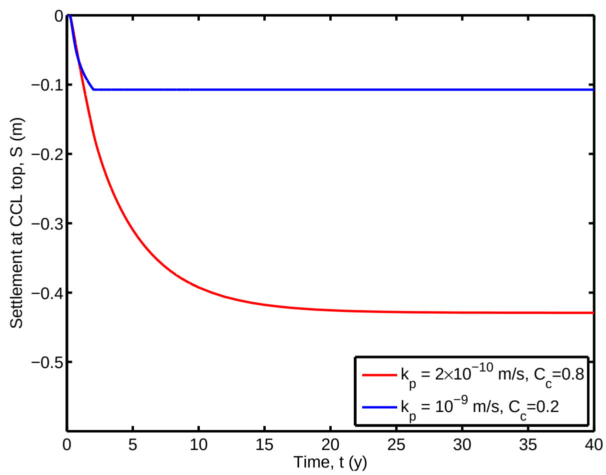

Figure 4: Consolidation settlements in a saturated soil ($S_r = 1$).

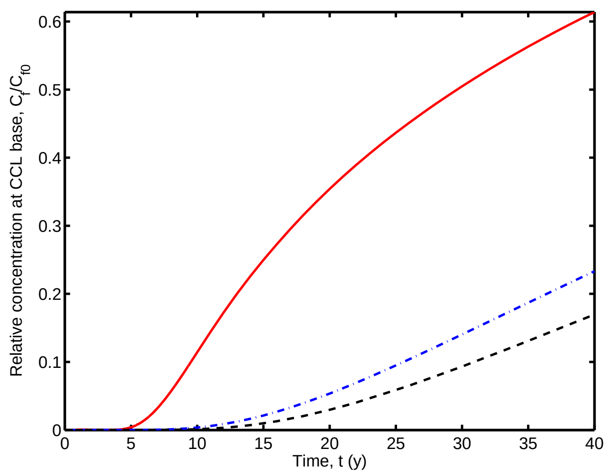

(a) $K_d = 0$

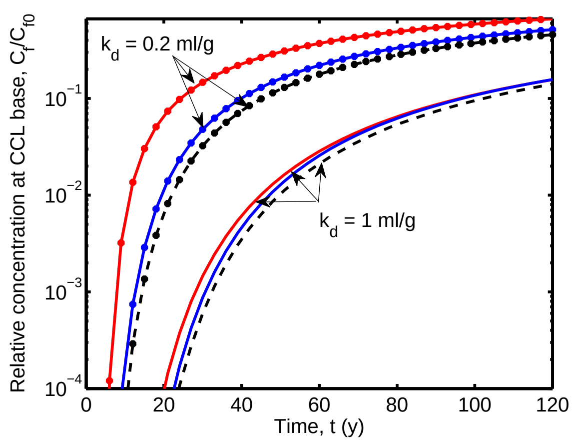

(b) $K_d \neq 0$

Figure 5: Effect of consolidation on relative concentration C_f/C_{f0} in a saturated soil (a) $K_d = 0$ and (b) $K_d \neq 0$ ($S_r = 1$, without CPW, $\alpha_L = 0$, constant D_e). Notations: solid line (FD, finite deformation model): $C_c = 0.8$, $k_p = 2 \times 10^{-10}$ m/s; dash-dot line (FD, finite deformation model): $C_c = 0.2$, $k_p = 10^{-9}$ m/s; and dashed line: no deformation model (ND).

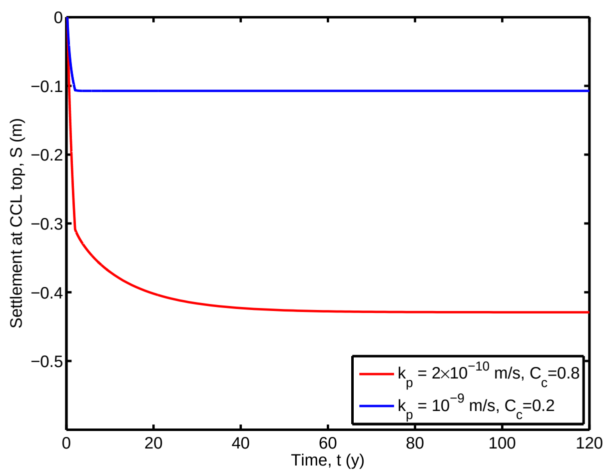

Figure 6: Consolidation settlement in partially saturated soils ($S_r = 0.8$).

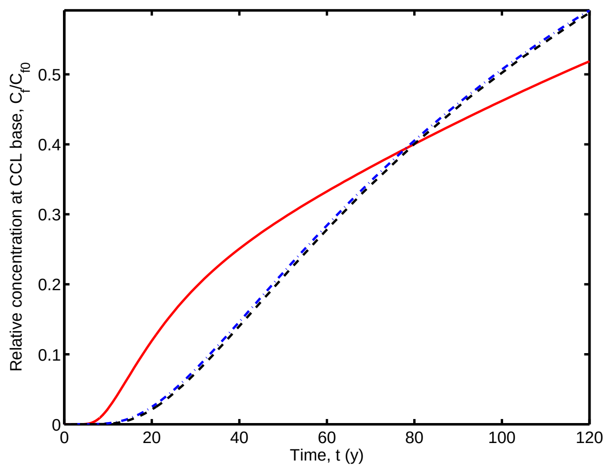

(a) $K_d = 0$

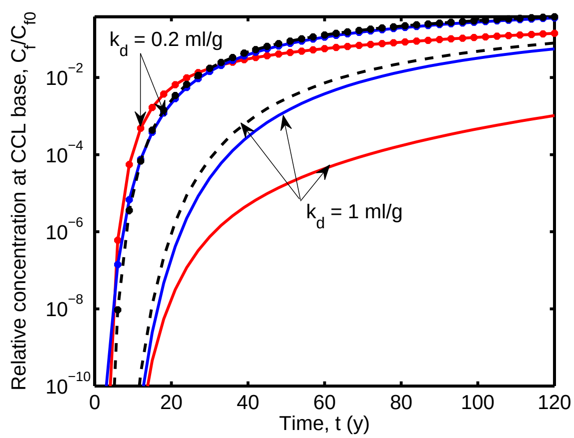

(b) $K_d \neq 0$

Figure 7: Effect of consolidation on relative concentration C_f/C_{f0} (a) $K_d = 0$ and (b) $K_d \neq 0$ in partially saturated soils ($S_r = 0.8$, with CPW, $\alpha_L = 0.1$ m, varying D_e as in Equation Eq. (33)). Notations: solid line (FD, finite deformation model): $C_c = 0.8$, $k_p = 2 \times 10^{-10}$ m/s; dash-dot line (FD, finite deformation model): $C_c = 0.2$, $k_p = 10^{-9}$ m/s; and dashed line: no deformation model (ND).

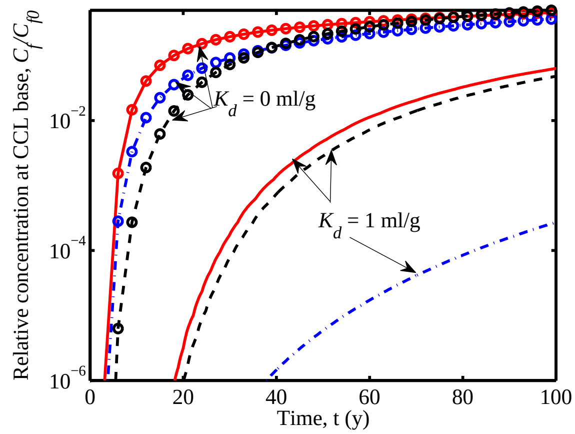

Figure 8: Effect of advection flux on concentration level at CCL base for partially saturated cases ($S_r = 0.8$, with CPW, $\alpha_L = 0.1$ m, varying D_e as in (33)). For finite deformation model, solid line: $C_c = 0.8$, $k_p = 2 \times 10^{-10}$ m/s; dash-dot line: without advection flux in transport, (20); dashed line: No deformation model.

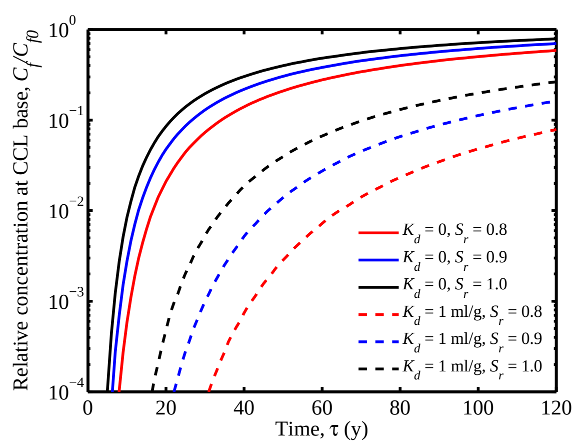

Figure 9: Effect of saturation S_r on transport for no-deformation model

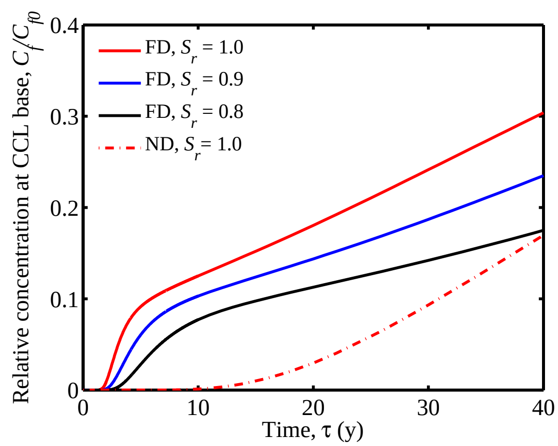

(a) $K_d = 0$

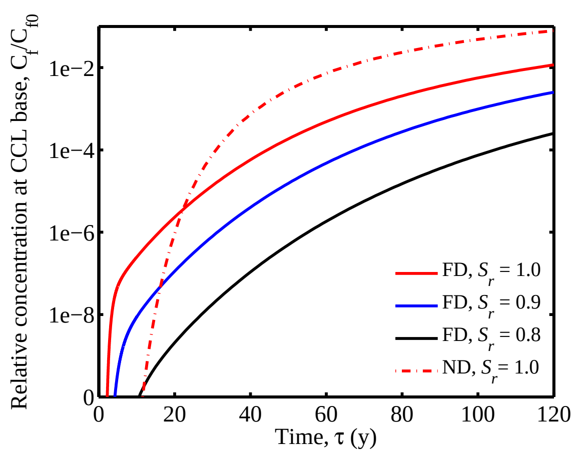

(b) K_d = 1 ml/g

Figure 10: Concentration level at CCL base for partially saturated cases with decreasing D_e. (C_c = 0.8, $k_p = 10^{-9}$ m/s). Notation: FD: finite deformation model and ND: no deformation model.

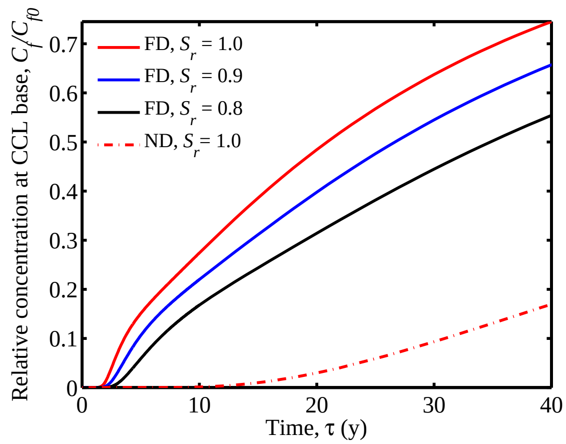

(a) $K_d = 0$

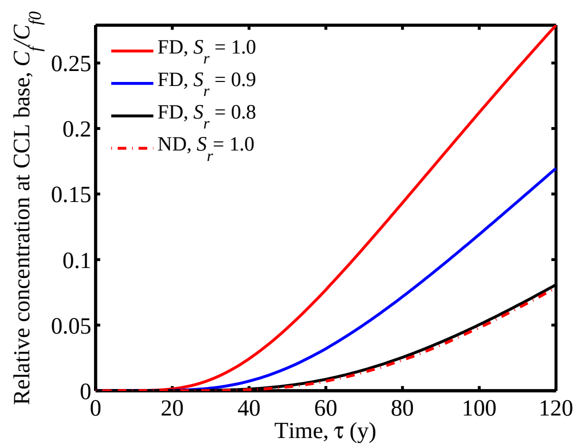

(b) $K_d = 1$ ml/g

Figure 11: Concentration level at CCL base for partially saturated cases with a constant D_e ($\theta = S_r n_0$ in (33)). ($C_c = 0.8$ and $k_p = 10^{-9}$ m/s). Notation: FD: finite deformation model and ND: no deformation model.

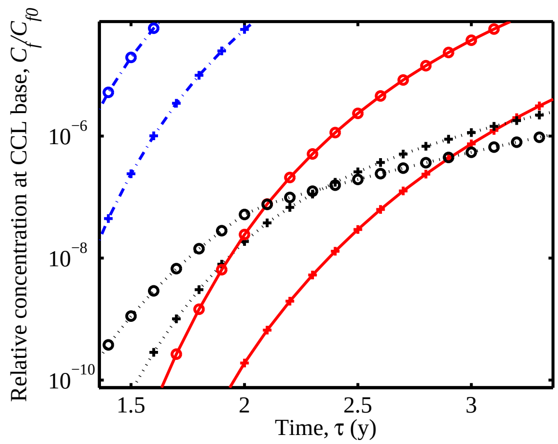

Figure 12: Effect of CPW on concentration level at CCL base for partially saturated cases (S_r = 0.8) with varying D_e and without sorption (K_d = 0). Solid lines: C_c = 0.8, k_p = 2×10^{-10} m/s; Dashdot lines: C_c = 0.8, k_p = 10^{-9} m/s; Dotted lines: C_c = 0.2, k_p = 10^{-9} m/s. Cross symbol: with CPW; circle symbol: without CPW ($\beta = 0$).

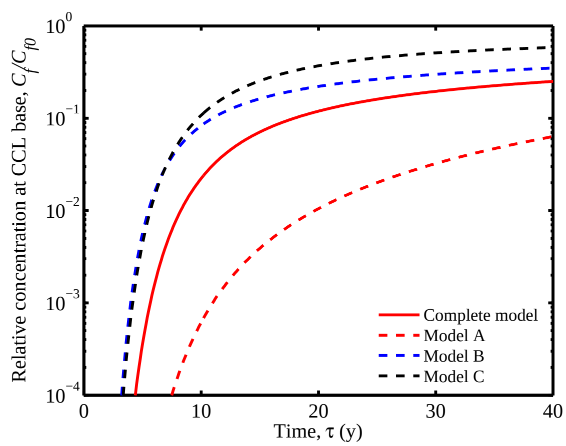

Figure 13: Significance of each term involving β on concentration level at CCL base for partially saturated cases (S_r = 0.8, C_c = 0.8, k_p = 2×10^{-10} m/s) with varying D_e and without sorption (K_d = 0).

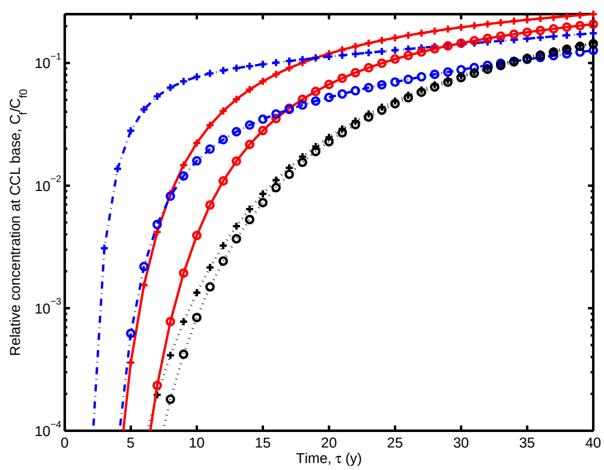

Figure 14: Effect of dispersion on concentration level at CCL base for partially saturated cases ($S_r = 0.8$) with varying D_e and without sorption ($K_d = 0$). Solid lines: $C_c = 0.8$, $k_p = 2 \times 10^{-10}$ m/s; Dashdot lines: $C_c = 0.8$, $k_p = 10^{-9}$ m/s; Dotted lines: $C_c = 0.2$, $k_p = 10^{-9}$ m/s. Cross symbol: $\alpha_L = 0.1$ m; circle symbol: $\alpha_L = 0$ (no dispersion).

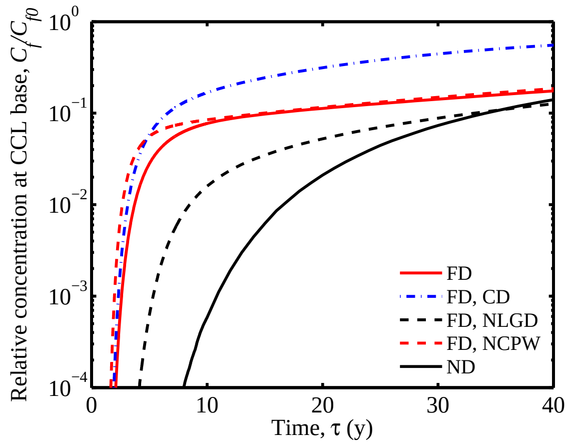

(a) $K_d = 0$

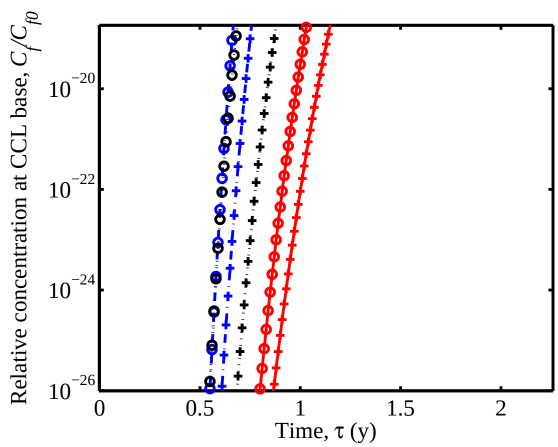

(b)K_d = 1 ml/g

Figure 15: Comparison of the concentration level at CCL base for various variable associative in partially saturation soils (S_r = 0.8, C_c = 0.8, $k_p = 10^{-9}$ m/s). Notation: FD: finite deformation model; CD: constant D_e; NLGD: excluding the dispersion; NCPW: excluding the CPW; ND: no deformation model.